Published in final edited form as:
Cancer Res. 2010 February 1; 70(3): 1033–1041. doi:10.1158/0008-5472.CAN-09-2113.

NEK4 STATUS INFLUENCES DIFFERENTIAL SENSITIVITY TO MICROTUBULE POISONS

Jason Doles[1] and **Michael T. Hemann**[1,2]

[1] The Koch Institute for Integrative Cancer Research at MIT, Massachusetts Institute of Technology, Cambridge, MA 02139, USA

Abstract

While microtubule poisons are commonly used for the treatment of diverse malignancies, relatively little is known about cellular factors that determine the relative efficacy of these drugs. Here, we identified the NIMA kinase, Nek4, in a genetic screen for mediators of the response to the front-line chemotherapeutic taxol. To identify the mechanism underlying taxol resistance in Nek4-deficient cells, we examined Nek4 function in mitosis and microtubule homeostasis. Notably, we found that Nek4 promotes microtubule outgrowth following transient depolymerization. Additionally, cells lacking Nek4 showed an impaired G2/M arrest following taxol treatment, as well as a decrease in mitotic-like asters, further suggesting a role for Nek4 in the regulation of microtubule assembly. Interestingly, Nek4 suppression also *sensitized* cancer cells to vincristine, another microtubule poison with a distinct mechanism of action. Therefore, Nek4 deficiency may either antagonize or promote the effects of microtubule poisons, depending on whether an individual drug hyper- or hypo-stabilizes microtubule polymers. While this phenomenon has previously been documented for cells bearing specific tubulin mutations, these data provide yet another example of how an alteration promoting drug resistance in a particular tumor can simultaneously enhance the efficacy of another, similar conventional chemotherapeutic. Of note, Nek4 is located in a commonly deleted genomic locus in non-small cell lung cancer. Consequently, these data also suggest a rationale for the selective use of particular microtubule poisons in specific lung cancer patients.

Keywords

Tubulin-targeted agents; animal models; novel mechanisms

INTRODUCTION

Microtubules are highly dynamic tubulin polymers crucial for the proper execution of numerous cellular processes. They play key roles in mitosis, promoting both mitotic spindle formation as well as the subsequent segregation of replicated DNA. Consequently, microtubules are an attractive anti-cancer target, as disruption of mitosis in highly proliferative cancer cells often results in cell death (1–5). Indeed, several classes of microtubule-disrupting drugs are currently used in clinical settings. Notably, the taxanes and the *vinca alkaloids* are front-line therapies in the treatment ovarian, breast, lung and certain hematopoietic malignancies. Unfortunately, acquired and intrinsic drug resistance significantly limits the efficacy of these agents (6–9).

[2]Corresponding author: Michael T. Hemann, Koch Institute for Integrative Cancer Research at MIT, Cambridge, MA 02139, hemann@mit.edu.

One of the most widely studied mechanisms of tumor cell survival following chemotherapy is multi-drug resistance (MDR), a phenotype involving decreased drug accumulation resulting from increased drug efflux (10,11). However, many tumors with inactive MDR still display resistance to microtubule poisons. Thus, multi-factorial or alternative mechanisms of resistance must exist. Indeed, a number of resistance-causing alterations at the drug-target interface have previously been described for tubulin, including genetic mutations, isotype selection, post-translational modification and altered regulation (12). Further, modifications in downstream signal transduction have also been suggested to contribute to microtubule-poison resistance (13–15). Still, major genetic factors underlying the efficacy of microtubule-targeting drugs, as well as the rationale for using one microtubule poison versus another, remain unclear.

In an effort to better understand the genetic basis of chemotherapeutic response to specific microtubule drugs, we performed an *in vitro* RNAi-based screen for mediators of the response to taxol, a commonly used microtubule-stabilizing taxane. This screen identified Nek4, a gene with unknown function belonging to a family of mitotic kinases termed NIMA-related kinases. Functional studies involving Nek4 showed that it has a role in microtubule regulation and that altered expression of this protein not only affected chemotherapeutic response, but also conferred differential sensitivity to select microtubule-disrupting drugs. Interestingly, Nek4 is frequently deleted in lung cancer, and Nek4 levels in several human cell lines correlated with differential sensitivity to microtubule poisons.

METHODS

Cell culture and chemicals

Eμ-myc mouse B-cell lymphomas were cultured in B-cell medium (45% DMEM/45% IMDM/ 10% FBS, supplemented with 2 mM L-glutamine and 5μM β-mercaptoethanol). Mouse and human lung adenocarcinoma cells were cultured in standard DMEM/FBS and RPMI/FBS medias, respectively. Chemotherapeutic agents were purchased from LC Laboratories (taxol) and Calbiochem (doxorubicin, vincristine, cisplatin, and 5-florouracil) and used at the indicated concentrations. For *in vivo* studies, vincristine (0.9% NaCl solution) and taxol (EtOH:Cremaphor:NaCl) were dissolved immediately prior to injection.

Retroviral constructs

shRNA constructs were designed and cloned as previously described (16). Sequences (5′-3′) targeted by shRNAs are as follows: shNek4-1 (Mm): GGAGAATCGTTGAAGTCTTAA, shNek4-2 (Mm): CACGTGGATGCCGCTGATGAA, shNEK4-1 (Hs): CAGCGTAAATATTGACATCTTA, shNEK4-4 (Hs): CTAAGGAGTAGTTGATAAATTA. Additional shRNA sequences are available upon request. Full-length human Nek4 cDNA was purchased from Open Biosystems (clone ID: 5169184) and cloned into a MSCV-based retroviral vector (pMIG). Cloning strategies and primer sequences are also available from the authors on request.

RNAi screening

Screening was performed using small pools (~48 shRNAs/pool) of the previously described ‘Cancer 1000’ shRNA library (16). For a given shRNA pool, approximately 2–4 million infected lymphoma cells (1–2 million uninfected cells/ml, 10ml on a 10cm tissue culture plate, ~20% infection efficiency) were subjected to taxol-based GFP enrichment assays (described below). shRNA identities in enriched pools were subsequently determined as previously described (16).

Western blotting, Immunofluorescence and RT-qPCR

For western blotting and RT-qPCR, protein or total RNA was isolated after retroviral infection and puromycin selection. RT-qPCR was performed using SYBR green on a BioRad thermal cycler. Nek4 mRNA levels were normalized to relative GAPDH mRNA abundance. Primer sequences are available upon request. For western blotting, cell lysates were prepared in lysis buffer (1% sodium deoxycholine, 0.1% SDS, 1% triton-X, 10 mM Tris-HCl, pH 8.0, 140 mM NaCl) for 10 minutes, cleared for 15 minutes at 14,000 rpm, then mixed with 5× SDS sample buffer. Proteins were then run on a 10% SDS-PAGE gel, transferred to PVDF (Millipore) and detected with the following antibodies: anti-Nek4 (Hahn Laboratory - Dana-Farber Cancer Institute, 1:250) and anti-GAPDH (Santa Cruz, 1:10000). Cells for immunofluorescence were grown and treated on poly-L-lysine coated coverslips, fixed with 100% methanol for 5 minutes at −20°C and stored for later use. Anti-α-tubulin [YL1/2] (Abcam, 1:2000) and anti-γ-tubulin (Sigma, 1:200) were used along with Alexa secondary antibodies (Molecular Probes) to visualize microtubules and centrosomes, respectively. Stained coverslips were imaged and analyzed using Applied Precision DeltaVision instruments and deconvolution software.

Flow Cytometry and cell cycle experiments

All assays were performed using Becton-Dickinson FACScan or MoFlo flow cytometers. Cell death was detected by propidium iodide (PI) incorporation (0.05 mg/mL), and dead cells were excluded from GFP analysis. Live cell sorting was performed using GFP co-expression as a marker of cell transduction. For phospho-histone H3/PI (cell cycle) assays, cells were fixed in 70% EtOH, then stained using an anti-pH3 antibody (Santa Cruz, 1:2500) followed by an Alexa (488) secondary antibody. Stained cells were then co-stained in a sodium citrate/PI buffer prior to FACS analysis.

GFP-competition and viability assays

For competition assays, lymphoma cells were partially transduced with the indicated shRNA constructs, treated with chemotherapeutic agents (taxol at 4, 6, and 8nM, doxorubicin at 10ng/ml, cisplatin at 7.5ng/ml, 5-fluorouracil at 40ng/ml and vincristine at 1.5nM), and monitored by flow cytometry for changes in the percentage of GFP+ cells. For viability assays, cells were plated subconfluently in 96-well plates, treated with drug (LA, colo669, H460, and H1395 cells were treated with 5μM taxol or 5μM vincristine and Sklu1 cells were treated with 0.04, 0.2, 1, 5, 25 and 125μM taxol or vincristine) and analyzed 48h post-treatment using CellTiter-Glo reagent (Promega) on an Applied Biosystems microplate luminometer.

In vivo mouse experiments

Syngeneic C57BL6/J female recipient mice were intravenously injected (via tail vein) with 4 million lymphoma cells and monitored until palpable tumors formed (~14 days). Upon tumor presentation, mice were administered either 25mg/kg taxol or 1.0 mg/kg vincristine (short-term enrichment studies) or 1.5mg/kg vincristine (long-term survival studies) intraperitoneally and monitored until the indicated timepoints, at which time mice were sacrificed and tumor material collected, if necessary.

Microtubule polymerization assay

Cells plated on poly-L-lysine coated coverslips were treated with 0.5 μM nocodazole for 30′ at 37°C/5% CO_2. Coverslips were briefly washed with PBS and allowed to recover for the indicated periods of time in nocodazole-free media at room temperature. Coverslips were then fixed using ice-cold methanol (5 minutes, −20°C) and stored in 4% BSA, 0.1% Triton-X, 0.05% sodium azide for subsequent immunofluorescent detection of α- and γ-tubulin. Microtubule length measurements were performed on representative images (5 fields/sample) using OpenLab5 (Improvision) software.

RESULTS

RNAi screen for modulators of taxol-induced cell death

We used cells from a well-established pre-clinical model of Burkitt's lymphoma, the *Eμ-myc* mouse, to screen a library of shRNAs (the Cancer 1000) for genes that promote the activity of the microtubule poison taxol. These shRNA-encoding vectors also expressed green fluorescent protein (GFP) to facilitate easy identification of transduced cells (17). shRNA pools were introduced into lymphoma cells by retroviral transduction, such that 20–30% of the target cells were infected, and were subsequently treated with taxol to enrich for shRNA-containing cells displaying enhanced drug resistance (Figure 1A). Using GFP-based flow cytometry to monitor the percentage of transduced (GFP-positive) lymphoma cells, we identified several pools that displayed GFP enrichment following treatment with taxol, indicating the presence of at least one resistance-conferring shRNA within each pool. Deconvolution of these enriched, post-treatment shRNA pools was performed using a previously described PCR/colony sequencing technique (18). Identification of known modulators of chemotherapeutic response (eg. p53) using our screening protocol suggested that this approach was sufficiently robust to identify contributors to the cellular response to taxol.

Nek4 is a modulator of microtubule poison-induced cell death

Examination of our enrichment data revealed an shRNA targeting Nek4 (shNek4) as a candidate suppressor of taxol-induced death. As an initial validation measure, shNek4 was isolated from the library and tested for the ability to promote taxol resistance as a single construct. As in our general screening strategy, a population of lymphoma cells was partially transduced with the shNek4 construct (co-expressing GFP), treated with taxol and analyzed by flow cytometry before and after treatment for changes in overall GFP percentage. In this context, shNek4-infected cells enriched relative to cells receiving a control vector. Additional shRNA constructs were then designed and tested to confirm this initial finding and address potential issues arising from well-documented 'off-target' RNAi effects (Figure 1B and Suppl. Table S1). Importantly, quantitative PCR analysis of Nek4 mRNA levels and western blotting for Nek4 protein in knockdown cells showed a correlation between the level of taxol resistance and the extent of target suppression (Figure 1C).

To determine how Nek4 suppression might promote resistance to taxol, we first examined whether Nek4 suppression conferred resistance to other, functionally distinct chemotherapeutic drugs. Here, we examined the response of shNek4-transduced cells to doxorubicin (a topoisomerase poison), cisplatin (a platinum-based DNA crosslinking agent), 5-fluorouracil (an antimetabolite) and vincristine (a microtubule destabilizer). To control for differential drug efficacy, cells were treated with drug doses that resulted in ~90% death at 48 hours. GFP-competition assays using the most potent Nek4 shRNA (shNek4-2) revealed no significant change in GFP percentage when treated with doxorubicin, cisplatin or 5-fluorouracil. Unexpectedly, Nek4 suppression *sensitized* lymphoma cells to treatment with vincristine, as evidenced by a depletion of GFP-positive shNek4-2 transduced cells following drug treatment (Figure 1D). Given that taxol and vincristine have opposing effects on microtubule stabilization, yet activate similar downstream checkpoints (19–21), these results suggested that Nek4 might promote or inhibit drug action directly at microtubules – as opposed to acting in a signaling network emanating from microtubule disruption.

Many regulators of microtubule dynamics have observable effects on cell cycle progression. Further, many chemotherapeutic agents preferentially affect actively cycling cells. To address the possibility that Nek4 suppression promotes taxol resistance by altering cell cycle progression, we determined the population growth rate, cell cycle profile (DNA content analysis), and mitotic index of shNek4-transduced cells. All three shNek4 populations were

indistinguishable from control cells in these experiments, suggesting that gross impairment of the cell cycle was not responsible for the taxol resistant phenotype (Table 1).

We next sought to determine if Nek4 status had any effect on microtubule poison-induced cell cycle profiles. For these experiments, we used a cell line derived from a previously described *LSL-Kras^{G12D}; p53$^{fl/fl}$* lung adenocarcinoma (LA) mouse model (22). These cells display a more protracted response to chemotherapy (as opposed to highly chemosensitive *Eμ-myc* lymphoma cells), allowing us to more clearly define subtle changes in the intermediate events preceding cell death. Importantly, we first confirmed that these cells also display opposing survival profiles in response to microtubule stabilizing versus destabilizing drugs (Figure 2A). Additionally, consistent with the data observed from untreated lymphoma cells, a comparison of 4N/2N DNA content ratios of untreated control versus shNek4-2 LA cells revealed little to no difference in cell cycle distribution (Figure 2B, first bar). However, in the presence of 5μM taxol, shNek4-2-transduced LA cells displayed a defective G2/M arrest relative to vector-infected controls. Conversely, vincristine treatment yielded a more pronounced accumulation of G2/M arrested cells in the absence of Nek4 (Figure 2B). Thus, the cellular status of Nek4 appears to impact the efficacy of microtubule poisons proximal to the drug/target interface.

Nek4 is involved in the regulation of microtubules following exposure to microtubule poisons

Exposure to taxol is known to have profound effects on microtubule organization, namely, the accumulation of mitotic-like asters and formation of abnormal microtubule bundles (23,24). Since precise microtubule phenotypes are known to vary from cell type to cell type (25), we first examined the impact of taxol on microtubules in lung adenocarcinoma cells. After a four-hour exposure to taxol, we found evidence of both mitotic-like asters and microtubule bundles in control cells. Under these conditions, the ‘aster’ phenotype predominated (Figure 3A and Suppl. Figure S1). Quantification of this phenotype in taxol treated control versus shNek4-transduced cell populations revealed a significant decrease in the percentage of cells harboring these aster-like structures: ~14% in Nek4-knockdown populations as compared to ~22% in controls (Figures 3A and 3B). Importantly, this effect was not simply dependent upon the number of cells available to form asters, as the mitotic index was not significantly different between the two cell populations - either in the absence or presence of taxol or vincristine (Figure 3b, right graph).

It has been previously reported that alterations in microtubule dynamics are associated with and can contribute to microtubule poison efficacy (26). Utilizing an established *in situ* microtubule polymerization assay, we examined whether Nek4-knockdown had any effect on microtubule repolymerization following nocodazole treatment. Cells were transiently exposed to nocodazole to depolymerize existing microtubules, washed with excess media to initiate repolymerization, and fixed, stained, and imaged at various time points to examine microtubule status. After a 30-minute incubation with nocodazole, microtubules were no longer detectable, as determined using α-tubulin immunofluorescence. While control cells showed rapid microtubule polymerization from centrosomes following nocodazole release, defects in microtubule assembly in Nek4-knockdown cells were apparent as early as one minute following release and clearly observable at the two-minute time point (Figures 3C and D). This suggests that impaired microtubule polymerization may underlie the differential sensitivity of Nek4-knockdown cells to taxol and vincristine.

Nek4 knockdown modulates microtubule poison efficacy *in vivo*

A strength of the *Eμ-myc* lymphoma model as a pre-clinical system is the ability to transplant genetically altered tumor cells into syngeneic, immunocompetent recipient mice, where the resulting disease is pathologically indistinguishable from lymphomas arising in germline *Eμ-myc* mice (27). This, along with the ability to specifically silence individual genes, allows for

rapid evaluation of putative regulators of chemotherapeutic response in an immunocompetent *in vivo* setting (Figure 4a). Utilizing this approach, we transplanted partially transduced control and shNek4-2 knockdown lymphomas into recipient mice and allowed palpable tumors to form (~14 days). Upon tumor presentation, mice were administered either 25mg/kg taxol or 1.0 mg/kg vincristine for 24hr, at which time tumor material was harvested for analysis by flow cytometry. In agreement with *in vitro* experiments, acute treatment of control tumors had no effect on the percentage of GFP-positive cells (not shown). In contrast, the percentage of GFP-positive shNek4-2 cells increased upon treatment with taxol, while selectively depleting when exposed to vincristine (Figure 4B). Further, mice harboring pure population (GFP sorted) shNek4-2 tumors showed an improved overall response to vincristine, with extended tumor-free and overall survival relative to their control counterparts (Figure 4c and data not shown).

Nek4 status modulates the relative sensitivity of human lung cancer cell lines to microtubule poisons

Microtubule poisons are front-line chemotherapies for the treatment of non-small cell lung cancer (NSCLC). Interestingly, many lung cancers harbor deletions on the short arm of chromosome 3 that include the Nek4 genomic locus. Thus, we reasoned that Nek4 status in NSCLC might contribute to the differential response of lung cancer cell lines to microtubule poisons. Given the complex constellation of mutations undoubtedly present across multiple cell lines, we limited our analysis to the relative sensitivity of cell lines to taxol versus vincristine. We tested several cell lines - one with a high level of Nek4 protein (colo669) and three (sklu1, H460, H1395) with reduced Nek4 levels. Interestingly, we found that colo669 cells had a significantly lower taxol versus vincristine (Tax/Vin) survival ratio – indicative of relative taxol sensitivity and/or vincristine resistance (Figure 5A). Importantly, shRNA-mediated knockdown of Nek4 in colo669 cells changed the response profile of these cells, promoting both taxol resistance and vincristine sensitivity (Figure 5B and Supplementary Table S2). Conversely, changes in drug sensitivity were not seen in a cell line expressing low levels of Nek4 (sklu1). However, overexpression of human Nek4 promoted vincristine resistance and sensitivity to multiple taxanes in sklu1 cells (Figure 5C and D). Thus, Nek4 levels in human cancers can significantly impact the relative sensitivity of these tumors to distinct microtubule poisons.

DISCUSSION

The founding member of the NIMA kinase family was first identified in an *Aspergillus nidulans* screen for mutants that were “Never In Mitosis” (28,29). Since then, 11 NIMA kinases have been identified by homology in mammalian cells. Four of these proteins, Nek2, Nek6, Nek7 and Nek9, have been shown to play roles in mitosis, while Nek1 and Nek8 are important for cilia function (30–32). Here, we show that Nek4 also plays a role in microtubule homeostasis. Importantly, however, this effect is only seen in the context of microtubule poisons. Multiple explanations could account for this effect. First, other proteins may compensate for Nek4 loss function during mitosis in untreated cells. Alternatively, partial Nek4 activity may be sufficient to allow for normal mitosis. While the shRNAs used in this study achieve near complete knockdown of Nek4 by western blot, it remains to be seen whether these vectors recapitulate Nek4 null phenotypes.

Interestingly, Nek4 deficiency results in resistance to taxol and sensitivity to vincristine. These data suggest that Nek4 functions at the level of microtubules, rather than on common downstream signal transduction pathways emanating from altered microtubule homeostasis. Given that at high drug doses, taxol is a microtubule-stabilizing agent and vincristine destabilizes microtubules, our data also suggests that Nek4 may play a role in promoting microtubule polymerization in the presence of drug. Consistent with this idea, Nek4 deficiency

impairs microtubule re-polymerization following nocodazole treatment. That a genetic alteration can confer opposite cellular responses to vincristine and taxol is not novel (33–36). Previous efforts in generating taxol-resistant cell lines have, in some instances, yielded cells that were vincristine sensitive (34,35,37). Notably, these studies highlighted the ability of tubulin mutations to confer differential sensitivity to microtubule poisons. Here, loss of function screening allowed for the identification of a regulator of therapeutic response that may have been overshadowed in these earlier efforts, presumably by more potent modifiers of the cellular response to microtubule poisons. Importantly, the effects of Nek4 manipulation on overall response to microtubule poisons are relatively minor, so further work will be required to determine whether pharmacological inhibition of Nek4 or associated proteins would have significant clinical benefit.

Interestingly, Nek4 is located in a genomic region that is commonly mutated in lung cancer. While it is unclear whether Nek4 is relevant to the pathogenesis of lung cancer, these data suggest a connection between the specific alterations that occur during lung cancer development and the ultimate response of that cancer to chemotherapy. Notably, the fact that Nek4 deficiency confers sensitivity to microtubule destabilizers suggests that existing therapies can be tailored towards this deficiency. For example, the combination of cisplatin and taxol are commonly used as a front-line therapy for non-small cell lung cancer. Our data suggests that a more personalized approach to treating lung cancer, utilizing vincristine rather than taxol in tumors with 3p deletions, may result in enhanced chemotherapeutic response.

Supplementary Material

Refer to Web version on PubMed Central for supplementary material.

Acknowledgments

We would like to thank William Hahn for generously providing us with the Nek4 antibody used in these studies. We would also like to thank Paul Chang for help with microtubule assays and members of the Hemann lab for helpful advice and discussions. M.T.H. is a Rita Allen Fellow and the Latham Family Career Development Assistant Professor of Biology and is supported by NIH RO1 CA128803-01. J.D. is supported by the MIT Department of Biology training grant.

References

1. Jordan MA, Wilson L. Microtubules and actin filaments: dynamic targets for cancer chemotherapy. Curr Opin Cell Biol 1998;10(1):123–30. [PubMed: 9484604]
2. Bhalla K, Ibrado AM, Tourkina E, Tang C, Mahoney ME, Huang Y. Taxol induces internucleosomal DNA fragmentation associated with programmed cell death in human myeloid leukemia cells. Leukemia 1993;7(4):563–8. [PubMed: 8096557]
3. Danesi R, Figg WD, Reed E, Myers CE. Paclitaxel (taxol) inhibits protein isoprenylation and induces apoptosis in PC-3 human prostate cancer cells. Mol Pharmacol 1995;47(6):1106–11. [PubMed: 7603448]
4. Martin SJ, Cotter TG. Disruption of microtubules induces an endogenous suicide pathway in human leukaemia HL-60 cells. Cell Tissue Kinet 1990;23(6):545–59. [PubMed: 2276172]
5. Woods CM, Zhu J, McQueney PA, Bollag D, Lazarides E. Taxol-induced mitotic block triggers rapid onset of a p53-independent apoptotic pathway. Mol Med 1995;1(5):506–26. [PubMed: 8529117]
6. Morris PG, Fornier MN. Microtubule active agents: beyond the taxane frontier. Clin Cancer Res 2008;14(22):7167–72. [PubMed: 19010832]
7. Kuppens IE. Current state of the art of new tubulin inhibitors in the clinic. Curr Clin Pharmacol 2006;1(1):57–70. [PubMed: 18666378]

8. Mechetner E, Kyshtoobayeva A, Zonis S, et al. Levels of multidrug resistance (MDR1) P-glycoprotein expression by human breast cancer correlate with in vitro resistance to taxol and doxorubicin. Clin Cancer Res 1998;4(2):389–98. [PubMed: 9516927]
9. Blade K, Menick DR, Cabral F. Overexpression of class I, II or IVb beta-tubulin isotypes in CHO cells is insufficient to confer resistance to paclitaxel. J Cell Sci 1999;112 (Pt 13):2213–21. [PubMed: 10362551]
10. Fojo T, Menefee M. Mechanisms of multidrug resistance: the potential role of microtubule-stabilizing agents. Ann Oncol 2007;18 (Suppl 5):v3–8. [PubMed: 17656560]
11. Bhalla K, Huang Y, Tang C, et al. Characterization of a human myeloid leukemia cell line highly resistant to taxol. Leukemia 1994;8(3):465–75. [PubMed: 7907395]
12. Orr GA, Verdier-Pinard P, McDaid H, Horwitz SB. Mechanisms of Taxol resistance related to microtubules. Oncogene 2003;22(47):7280–95. [PubMed: 14576838]
13. Blagosklonny MV, Fojo T. Molecular effects of paclitaxel: myths and reality (a critical review). Int J Cancer 1999;83(2):151–6. [PubMed: 10471519]
14. Strobel T, Swanson L, Korsmeyer S, Cannistra SA. BAX enhances paclitaxel-induced apoptosis through a p53-independent pathway. Proc Natl Acad Sci U S A 1996;93(24):14094–9. [PubMed: 8943066]
15. Barboule N, Chadebech P, Baldin V, Vidal S, Valette A. Involvement of p21 in mitotic exit after paclitaxel treatment in MCF-7 breast adenocarcinoma cell line. Oncogene 1997;15(23):2867–75. [PubMed: 9419978]
16. Burgess DJ, Doles J, Zender L, et al. Topoisomerase levels determine chemotherapy response in vitro and in vivo. Proc Natl Acad Sci U S A 2008;105(26):9053–8. [PubMed: 18574145]
17. Hemann MT, Fridman JS, Zilfou JT, et al. An epi-allelic series of p53 hypomorphs created by stable RNAi produces distinct tumor phenotypes in vivo. Nat Genet 2003;33(3):396–400. [PubMed: 12567186]
18. Dickins RA, Hemann MT, Zilfou JT, et al. Probing tumor phenotypes using stable and regulated synthetic microRNA precursors. Nat Genet 2005;37(11):1289–95. [PubMed: 16200064]
19. Masuda A, Maeno K, Nakagawa T, Saito H, Takahashi T. Association between mitotic spindle checkpoint impairment and susceptibility to the induction of apoptosis by anti-microtubule agents in human lung cancers. Am J Pathol 2003;163(3):1109–16. [PubMed: 12937152]
20. Sudo T, Nitta M, Saya H, Ueno NT. Dependence of paclitaxel sensitivity on a functional spindle assembly checkpoint. Cancer Res 2004;64(7):2502–8. [PubMed: 15059905]
21. Wang X, Jin DY, Wong HL, Feng H, Wong YC, Tsao SW. MAD2-induced sensitization to vincristine is associated with mitotic arrest and Raf/Bcl-2 phosphorylation in nasopharyngeal carcinoma cells. Oncogene 2003;22(1):109–16. [PubMed: 12527913]
22. Kim CF, Jackson EL, Kirsch DG, et al. Mouse models of human non-small-cell lung cancer: raising the bar. Cold Spring Harb Symp Quant Biol 2005;70:241–50. [PubMed: 16869760]
23. Rowinsky EK, Donehower RC, Jones RJ, Tucker RW. Microtubule changes and cytotoxicity in leukemic cell lines treated with taxol. Cancer Res 1988;48(14):4093–100. [PubMed: 2898289]
24. Schatten G, Schatten H, Bestor TH, Balczon R. Taxol inhibits the nuclear movements during fertilization and induces asters in unfertilized sea urchin eggs. J Cell Biol 1982;94(2):455–65. [PubMed: 6125518]
25. Gascoigne KE, Taylor SS. Cancer cells display profound intra- and interline variation following prolonged exposure to antimitotic drugs. Cancer Cell 2008;14(2):111–22. [PubMed: 18656424]
26. Goncalves A, Braguer D, Kamath K, et al. Resistance to Taxol in lung cancer cells associated with increased microtubule dynamics. Proc Natl Acad Sci U S A 2001;98(20):11737–42. [PubMed: 11562465]
27. Schmitt CA, Rosenthal CT, Lowe SW. Genetic analysis of chemoresistance in primary murine lymphomas. Nat Med 2000;6(9):1029–35. [PubMed: 10973324]
28. Morris NR. Mitotic mutants of Aspergillus nidulans. Genet Res 1975;26(3):237–54. [PubMed: 773766]
29. Osmani SA, May GS, Morris NR. Regulation of the mRNA levels of nimA, a gene required for the G2-M transition in Aspergillus nidulans. J Cell Biol 1987;104(6):1495–504. [PubMed: 3294854]

30. O'Regan L, Blot J, Fry AM. Mitotic regulation by NIMA-related kinases. Cell Div 2007;2:25. [PubMed: 17727698]

31. Quarmby LM, Mahjoub MR. Caught Nek-ing: cilia and centrioles. J Cell Sci 2005;118(Pt 22):5161–9. [PubMed: 16280549]

32. Parker JD, Bradley BA, Mooers AO, Quarmby LM. Phylogenetic analysis of the Neks reveals early diversification of ciliary-cell cycle kinases. PLoS ONE 2007;2(10):e1076. [PubMed: 17957258]

33. Ong V, Liem NL, Schmid MA, et al. A role for altered microtubule polymer levels in vincristine resistance of childhood acute lymphoblastic leukemia xenografts. J Pharmacol Exp Ther 2008;324 (2):434–42. [PubMed: 17986648]

34. Minotti AM, Barlow SB, Cabral F. Resistance to antimitotic drugs in Chinese hamster ovary cells correlates with changes in the level of polymerized tubulin. J Biol Chem 1991;266(6):3987–94. [PubMed: 1671676]

35. Kavallaris M, Burkhart CA, Horwitz SB. Antisense oligonucleotides to class III beta-tubulin sensitize drug-resistant cells to Taxol. Br J Cancer 1999;80(7):1020–5. [PubMed: 10362110]

36. Kavallaris M, Tait AS, Walsh BJ, et al. Multiple microtubule alterations are associated with Vinca alkaloid resistance in human leukemia cells. Cancer Res 2001;61(15):5803–9. [PubMed: 11479219]

37. Ohta S, Nishio K, Kubota N, et al. Characterization of a taxol-resistant human small-cell lung cancer cell line. Jpn J Cancer Res 1994;85(3):290–7. [PubMed: 7514586]

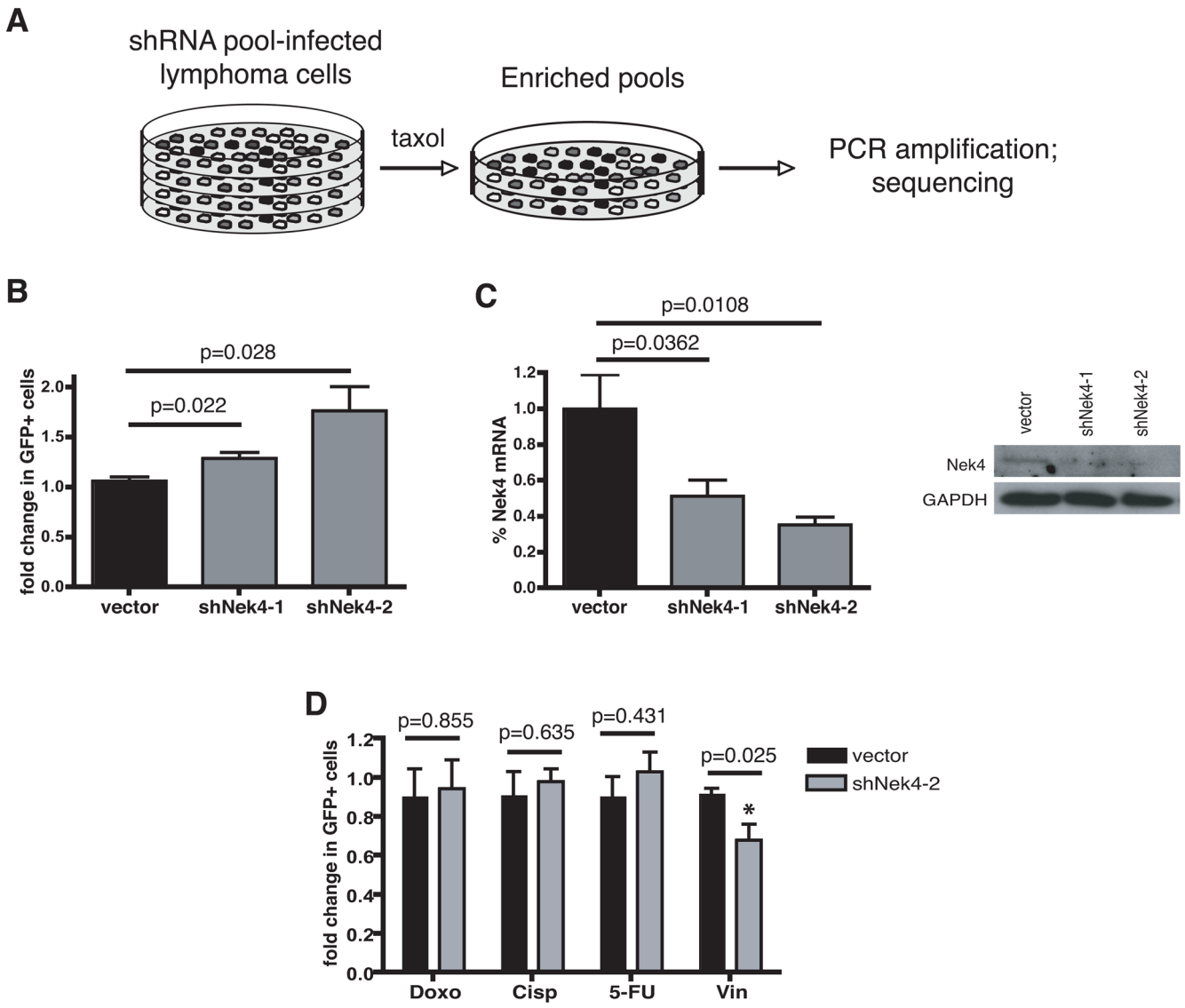

Figure 1. RNAi screening identifies Nek4 as a regulator of microtubule poison-induced cell death

(A)*In vitro* screening methodology. Lymphoma cells were partially infected with 48 pools of 48 distinct shRNAs, treated with taxol (4, 6, and 8nM) and monitored using GFP-based flow cytometry for changes in the relative percentage of shRNA-containing (GFP+) cells. Genomic DNA from enriched pools was subsequently subjected to shRNA-specific PCR and sequenced to determine relative shRNA abundance. **(B)** An *in vitro* GFP competition assay comparing relative taxol sensitivity in cells infected with two distinct shRNAs targeting Nek4 (6nM taxol, 48h post-treatment; n=5 for all samples). **(C)** qRT-PCR (n≥3) and western blot analysis of Nek4 expression in lymphoma cells. **(D)** Partially-transduced lymphoma cells were separately treated with doxorubicin (10ng/ml), cisplatin (7.5ng/ml), 5-fluorouracil (40ng/ml) and vincristine (1.5nM) at similar levels of cytotoxicity (~90% cell death at 48h). The percentage of GFP+ cells was determined 48 hours post treatment (n=3 for doxorubicin, 5-FU, cisplatin, and n=5 for vincristine treatments). Values are shown with standard deviations (s.d.). P-values were determined using a Student's *t*-test.

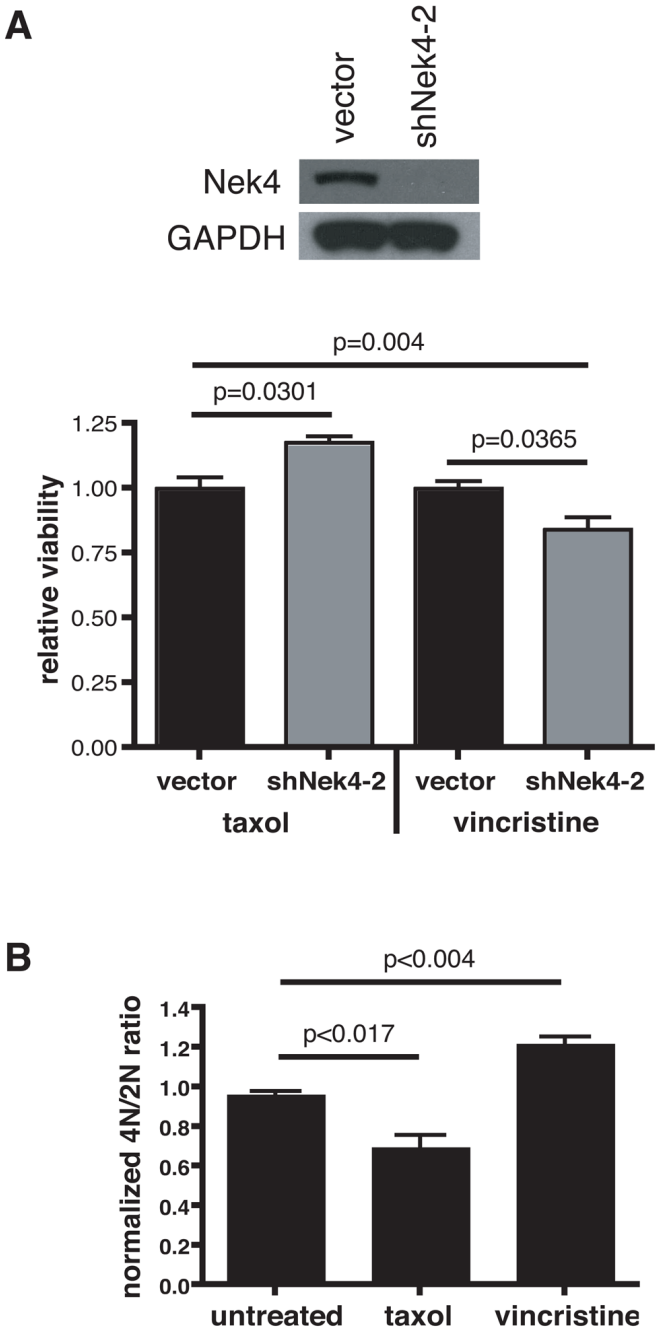

Figure 2. Nek4 knockdown promotes resistance to taxol, while sensitizing cells to vincristine

(A) (Above) A western blot showing Nek4 knockdown in lung adenocarcinoma cells expressing shNek4-2. (Below) shNek4-2 transduced cells were treated with 5μM taxol or vincristine and monitored for cell survival relative to cells expressing a vector control (n=3 independently treated samples for each drug, +/− s.d.). **(B)** G2/M arrest profiles in lung adenocarcinoma cells expressing shNek4-2. Knockdown cells were treated with 5μM taxol or 5μM vincristine for 8 hours and analyzed for DNA content by flow cytometry to determine the extent of the microtubule poison-induced G2/M arrest. Shown is the 4N/2N ratio (indicative of an arrest) normalized to matched vector control cells (n=3 for all samples +/− s.d.). P-values were determined using a Student's *t*-test.

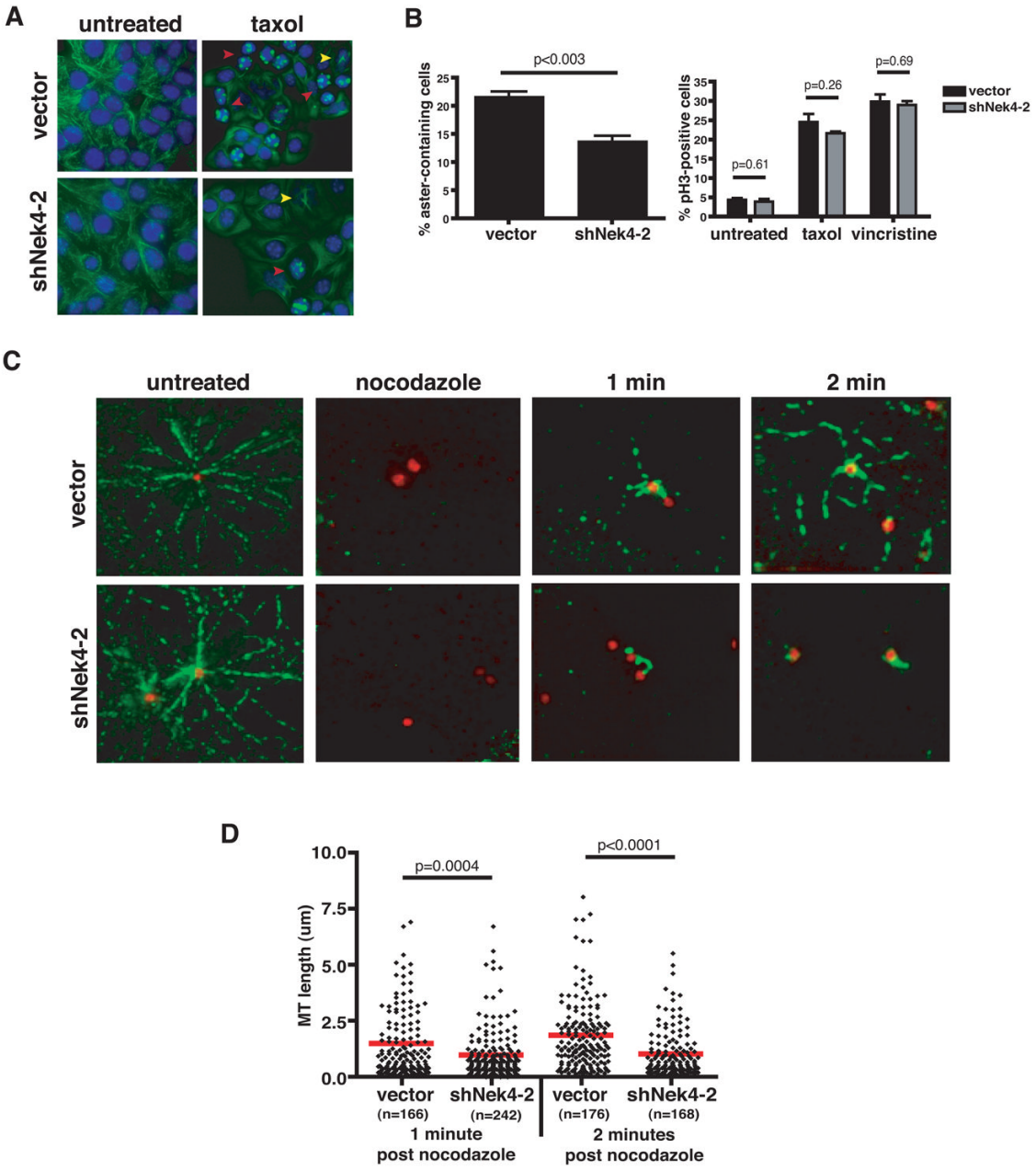

Figure 3. Nek4 knockdown cells show altered microtubule phenotypes

(A) LA cells expressing a Nek4 shRNA or a control vector were treated with 5μM taxol for 4h and then stained with anti-α-tubulin to visualize microtubules. Microtubule asters (red arrowheads) and bundles (yellow arrowheads) were observed under these conditions. **(B)** (Left graph) Quantification of aster containing cells in shNek4 and vector control infected cell populations using OpenLab5 software (n=3 independently treated replicates, 6 averaged fields/sample). (Right) Phospho-histone H3 staining of drug treated LA cells failed to show any significant change in the mitotic index in the presence or absence of Nek4 (n=3 for all samples +/− s.d.). **(C)** In a microtubule repolymerization assay, lung adenocarcinoma cells were allowed to repolymerize microtubules following transient (0.5μM, 30 minutes) nocodazole treatment. Qualitative differences were apparent at one (third column) and two (fourth column) minutes post-nocodazole release. **(D)** Quantification of the repolymerization defect in shNek4-2 LA

cells. Microtubule lengths are shown at the one and two-minute time points, respectively. The average microtubule length in each sample is indicated with a red bar. P-values were determined using a Student's *t*-test.

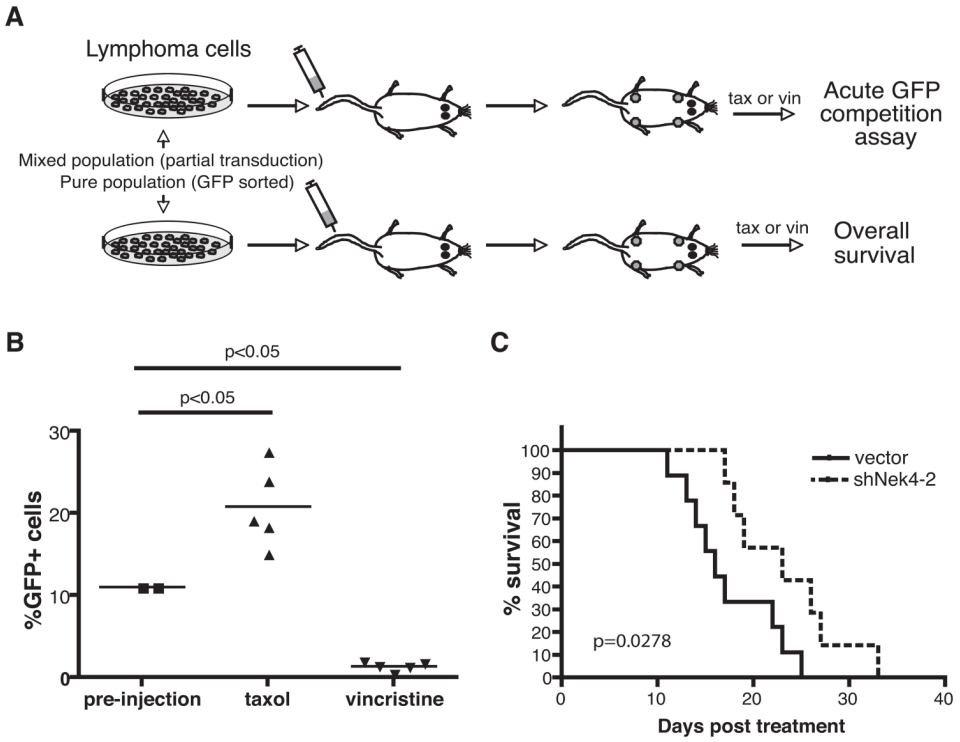

Figure 4. Nek4 suppression alters the response to microtubule poisons *in vivo*

(A) Schematic depicting *in vivo* experimental approaches. Partially transduced (upper row) or GFP-sorted (lower row) lymphoma cells were injected into recipient mice and allowed to develop into palpable lymphomas. Resulting tumors were then treated with taxol or vincristine and then either harvested to examine the percentage of GFP+ cells or monitored for tumor-free and overall survival rates. **(B)** Partially transduced shNek4-2 lymphomas were harvested 24 hours post drug treatment (25mg/kg taxol or 1.0mg/kg vincristine) and analyzed by flow cytometry for changes in GFP percentage. Taxol treatment resulted in an increase in the percentage of GFP+ cells (compared to pre-injection GFP levels), while vincristine-treated tumors displayed dramatic selection against Nek4 knockdown. P-values were determined using a Student's *t*-test **(C)** Kaplan-Meier survival curve depicting overall survival of shNek4-2 or control tumor bearing mice following treatment with a maximally tolerated dose (1.5mg/kg) of vincristine (vector, n=13; shNek4-2, n=12). P-values were determined using a log rank test.

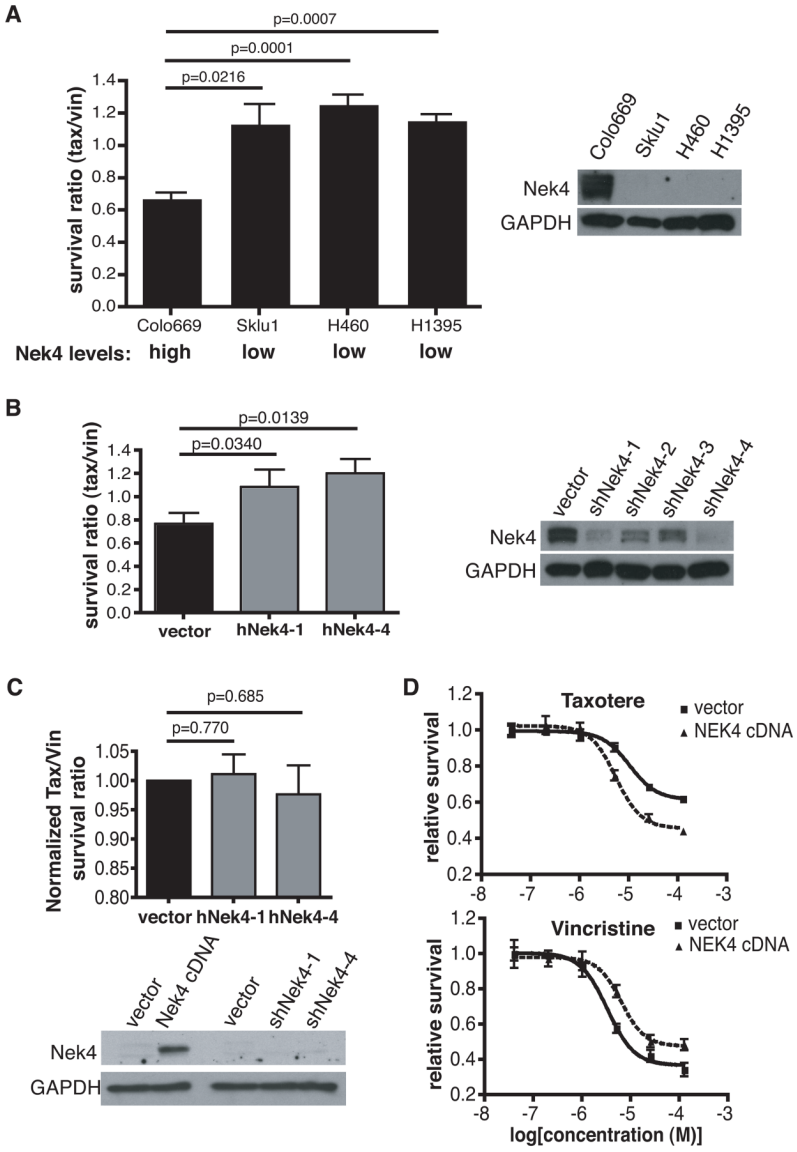

Figure 5. Nek4-dependent differential sensitivity to microtubule poisons in human lung adenocarinoma cells

(A) Four human lung adenocarcinoma cell lines were separately treated with taxol and vincristine and examined for viability 48 hours after treatment. Viability comparisons (left, graph) at a fixed drug dose of 5μM taxol or vincristine revealed one cell line (colo669) with a significantly lower taxol/vincristine survival ratio. This cell line also had high baseline levels of Nek4 protein (right, western blot). **(B)** Colo669 cells were retrovirally infected with shRNAs targeting human Nek4 and subjected to *in vitro* survival assays. Knockdown cells with significant depletion of Nek4 protein (right, western blot) also demonstrated relative resistance to taxol and sensitivity to vincristine (left, shown as an upward shift in the taxol/vincristine survival ratio). **(C)** Transduction of 'low-Nek4' sklu1 cells with Nek4 shRNAs did not affect their relative sensitivity to taxol and vincristine. (below) Western blot showing Nek4 levels following transduction of sklu1 cells with Nek4 shRNAs or a Nek4 cDNA. (D) Sklu1 cells stably overexpressing full length Nek4 cDNA were treated with either taxotere or vincristine for 48h, at which time cell viability was assessed using CellTiterGlo reagents. Mann-Whitney statistical comparison of EC50 values derived from best-fit non-linear regression curves

revealed increased sensitivity (avg. EC50 for vector control=10.5μM and NEK4=5.5μM, p=0.002) to taxotere and resistance to vincristine (avg. EC50 for vector control=3.3μM and NEK4=6.4μM, p=0.002) in cells overexpressing Nek4. Data was generated from three independent experiments for each drug.

Table 1

Cell cycle analysis of shNek4 infected *Eμ-myc* lymphoma cells

Actively cycling knockdown cell populations were fixed, stained with anti-phospho histone H3/propidium iodide, and analyzed by flow cytometry to determine the mitotic index (shown as % phospho histone H3 cells), and relative DNA content (shown as a ratio of 4N/2N cells). n=3 independently infected cell populations for each vector +/− s.d.

	4N/2N ratio (PI)	Mit Index (pH3+)	Doubling time (h)
vector	0.51+/−0.07	3.7+/−0.4	8.3+/−0.4
shNek4-1	0.46+/−0.5	3.5+/−1.2	8.4+/−0.8
shNek4-2	0.45+/−0.02	3.2+/−0.4	8.0+/−0.7
shNek4-3	0.5+/−0.06	3.9+/−0.6	8.7+/−1.0